LIGHTWEIGHT STRUCTURES in CIVIL ENGINEERING
CONTEMPORARY PROBLEMS
Monograph from Scientific Seminar
Organized by Polish Chapters of
International Association for Shell and Spatial Structures
Lodz University of Technology
Faculty of Civil Engineering, Architecture and Environmental Engineering
XXIV LSCE
Łódź, 7th of December 2018 (Friday)

FRICTION SLIDING BEARING IN ENGINEERING STRUCTURES

I. Gołębiowska[1)] M. Dutkiewicz[2)] B. Usewicz [3)]
[1)] Professor, [2)] Adjunct Professor, [3)] Specialist, Faculty of Civil Engineering, Architecture and Environmental Engineering, University of Sciences and Technology in Bydgoszcz, Poland, macdut@utp.edu.pl

ABSTRACT: The paper focuses on the analysis of currently selected and tested sliding base isolation bearings. Three types of passive adaptive sliding bearings have been described succinctly, which are stable and effective at each type of earthquake, comparing to conventional sliding friction bearings. Each of these devices has a unique way of dissipating anergy and controlling the vibrations. The results of the analysis of literature show that engineers can control the level of constructions' vibrations with proper application of adaptive sliding bearings.

Keywords: sliding base isolation, passive adaptive seismic bearing, vibration reduction, vibration control

1. INTRODUCTION

Dynamic loads acting on various construction objects, buildings and infrastructure elements, in many cases require mechanical applications of vibration reduction systems that effectively limit the disbeneficial effects of these loads (Refs 1-12). A special group of vibration reduction devices are seismic isolation.

Seismic isolation systems are isolation devices that are placed between a structure and it's foundation to protect it from damage due to earthquake shaking. Simplistically, seismic isolation reduces response of the superstructure by decoupling the structure from seismic ground motion. Typical isolation systems reduce the seismic forces transmitted to the superstructure by extending the vibration period of the structure and adding some amount of damping. This attenuation is an inherent feature of many modern isolators / bearings, but it can also be provided by additional energy dissipation devices mounted across the isolation interface e.g. viscous dampers, friction dampers, yielding dampers, etc. (Refs 13-15). These additional damping devices used in combination with isolators help them keep the structure to a pre-shock position and increase resistance. The extension of the vibration period of the structure results in an increase in displacements and a reduction in the acceleration of the structure. Accelerations are reduced, but the level of their reduction depends on the force-displacement of the isolator.

There are many different seismic isolation bearings, which are constantly improved and widely applied in various engineering constructions, eg. in buildings, bridges, tanks, industrial facilities. These isolating devices can essentially be divided into two groups: elastomeric and sliding bearings. Elastomeric bearings use elastic properties of rubber to isolate structures from harmful vibrations of the ground, while sliding bearings are characterized by low rigidity and friction at the interface, mostly between stainless steel and teflon (polytetrafloroethylene - PTFE).

Isolation devices should have the following properties:

- high axial rigidity (for transferring vertical loads without excessive deformation),
- sufficiently low horizontal stiffness, so that the first natural frequency of the isolated structure is significantly lower than the predominant frequency of expected ground movement,
- restoring force and re-centering capacity to reduce residual displacement,
- effective mechanism of energy dissipation, contributing to the reduction of excessive horizontal (lateral) displacements.

The basic principle of sliding bearings is the implementation of low horizontal stiffness and the dissipation of energy in these devices occurs on the sliding interface through Coulomb's friction. The objective of a engineer who designs seismic base isolation is to maximisation of a period and maximisation of damping (with displacement control) at the same time.

The paper presents a review of the most important friction sliding bearings used in engineering objects exposed to seismic influences, in the context of their effectiveness.

2. CONVENTIONAL SLIDING SUPPORTS

The basic sliding supports include - Pure-Friction (PF) bearing without any restoring force and the Friction Pendulum (FP) bearing. PF bearing works with the principle of pure friction. It is the simplest of all sliding isolation systems. Two horizontal flat stainless steel plates slide one on another. The upper plate slides on the lower plate under force excitation. The structure resting on the upper plate moves during the earthquake like a rigid body. A prerequisite for starting the isolator is that the forcing force is greater than the friction force of the isolator. As the isolator surface is horizontal, its radius of curvature is infinite and therefore it has no defined period of natural vibration. Therefore, the frequency of excitation caused by the earthquake will never be equal to the frequency of the isolator, and therefore this isolator will not

experience resonance frequency. The maximum horizontal force transferred to the superstructure is in the form (Fig 1):

$$F_{max} = \mu W \operatorname{sgn}(\dot{x}), \tag{1}$$

where: W is the normal force acting on the isolator, μ is the sliding coefficient of friction and $\dot{x}$ is the sliding velocity of the isolator.
The energy dissipated per cycle E at the design displacement d is (Fig. 1):

$$E = 4\mu W d. \tag{2}$$

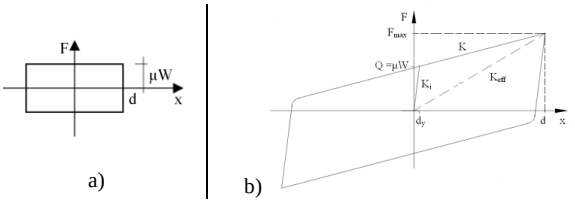

Fig.1 Sliding friction hysteric behavior for: a) flat and b) curved surfaces

Due to the possible substantial permanent offset displacements PF bearing should be used in combination with devices providing required adequate restoring force.
The Frictional Pendulum (FP) bearing (or single concave friction pendulum (SCFP) bearing) was first proposed by Zayas at all (Ref. 16). The FP bearing is a sliding device based on the principle of the pendulum motion. This device combines two basic mechanisms– pendulum motion of the slider on a spherical surface and the frictional sliding of steel surfaces, so restoring mechanism and energy dissipation mechanism. The FP bearing consists of a base-plate, an articulated slider, covered by the PTFE – type composite material, and spherical concave dish (stainless steel) (Fig. 2 - Fig. 4). The sliding surface can have a restraining rim around the edge to limit the displacement. Under the influence of horizontal movement the spherical concave dish moves horizontally relative to the base-plate and the slider.

Fig.2 Concave, slider & housing for FP bearing (Ref. 17)

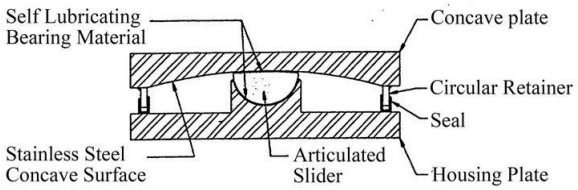

Fig.3 Friction Pendulum system (Ref. 18)

The device can be either mounted in an upward or downward position (Fig 4).
These are equivalent positions for isolating effects, but different for design, i.e. downward, the P-Δ effect is transmitted to the structure below the isolation system, usually to the foundation. If the FP bearing is in the upward position, the same P-Δ effect is transferred to the resisting elements of the superstructure.
The unidirectional horizontal force displacement response of the FP bearing is given by:

$$F = W\left[\frac{x}{R} + \mu \operatorname{sgn}(\dot{x})\right], \tag{3}$$

where: W is the normal force of the isolator, R is the radius of the spherical curvature, x is horizontal displacement of the pivot point of the slider and $\dot{x}$ is the sliding velocity.

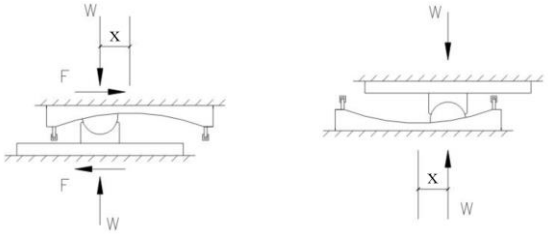

Fig. 4 Modelling of FP bearings a) bearing in upward position, b) bearing in downward position (Ref. 17)

The effective damping provided by a frictional isolator is equal:

$$\xi_{eff} = \frac{2}{\Pi}\left[\frac{\mu}{\mu + d/R}\right]. \tag{4}$$

The sliding interface is designed with a low coefficient of friction, which limits the resistance to horizontal forces. The lateral restoring force is provided through spherical shape of the sliding surface. The lateral restoring stiffness of the bearing providing the restoring capability of the system is determined by $K = W/R$.
FP bearing uses the characteristics of the pendulum to extend the natural vibration period of the isolated structure. This period is designed based on the radius of curvature of the surface, it is independent of the mass of supported structure and is equal:

$$T = 2\Pi\sqrt{R/g}, \quad T_{eff} = 2\Pi\sqrt{\frac{m}{K_{eff}}}, \tag{5}$$

where g is the gravity acceleration, m is the mass on the bearing and $K_{eff} = F_{max}/d$.
The restoring stiffness which is proportional to the curvature of the sliding surface will introduce a constant isolation frequency (constant isolation natural period) to the isolated structure.
Therefore, resonance problems may occur when the FP bearing is subjected to strong - long components of an earthquake (near - fault ground motion). Hence, the system requires design for a strictly defined level of excitation. Torsional motion of the structure is minimized, because the center of bearing stiffness (bearing) automatically coincides with the centre of mass of the structure.
For constant values of axial load and sliding friction coefficient, the force-displacement relation in the horizontal direction can be described by a bilinear hysteretic relationship. The hysteretic loop of FP bearing is approximately rigid plastic with post yielding hardening (Fig. 1b). Three parameters

– the characteristic strength Q is given by Q=μW,
– the post-elastic stiffness determined as K=W/R,
– the initial elastic stiffness K_i,

characterize the hysteresis loop of the FP bearing.
The hysteresis loop is more complicated, it depends on many factors, of which the normal force is the main factor. Actual constitutive law for FP bearing is an elastic-plastic type with strain hardening resulting in a hysteresis loop extremaly varying from the standard constant shape.

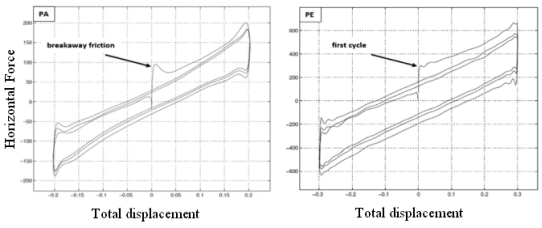

Fig. 5 Force-displacement hysteresis responses for PA and PE based FP bearing (Ref. 19)

Figure 5 shows two typical hysteresis loops for two different materials covering slider - polyamide (PA) and polyethylene (PE). In response, force-displacement for PA has a clear stick-slip effect at the breakaway and load reversal, while for PE the effect is much smaller (similar to PTFE materials) (Ref. 19). The sliding friction coefficient changes its value during an earthquake along with the sliding velocity, axial pressure and the temperature on the slip surface (Fig. 6).

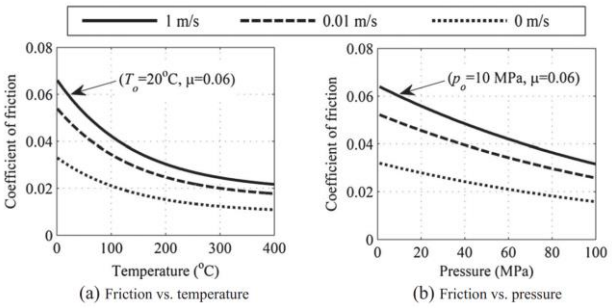

Fig. 6 Variation in the coefficient of sliding friction with sliding velocity, axial pressure and temperature at the sliding surface (Ref. 20)

Figure 6 shows the dependence of the coefficient of friction on speed, temperature and pressure. The temperature at the sliding surfaces at a given moment depends on the sliding speed, axial pressure, coefficient of friction and path traveled by the slider. Due to the viscosity of the composite (PTFE type) used for the liner, the sliding speed affects the coefficient of friction. This coefficient increases with the increase of the sliding speed up to a fixed value. The coefficient of friction at high speeds increases considerably with increasing axial pressure, while at low speeds this coefficient changes little. The coefficient of friction decreases sharply as the temperature rises, at lower temperatures, due to changes in the viscoelastic properties of the composite material (type PTFE), while at higher temperatures the degree of reduction of the coefficient is smaller and tends to a constant value.

The influence of the temperature increase on the response of construction isolated by slider bearings will be greater for bearings consisting of one surface and smaller for bearings with multiple sliding surfaces, for a given bearing pressure and liner material, due to the fact that heat flux separates into more than one sliding surface. Changes in the properties of the PTFE-type liner are related to heat and consequently changes in the coefficient of friction are a function of the slider path on the sliding surface and the temperature on the sliding surface directly beneath the slider. Expressions specifying the relationship between frictional coefficients and slip velocity, axial pressure and temperature were developed on the basis of experimental data and presented in (Ref. 20).

Lomiento et all (Ref. 21) identifies, based on a large set of experimental data, four main effects related to the frictional performance of the FP bearing, responsible for changing the rectagular friction coefficient - displacement loop:

1. breakaway effect - the sudden increase μ at the beginning of each motion and at each direction reversal,
2. load effect - the reduction μ for increasing contact pressure,
3. cycling effect - the continued reduction of μ with the fast repetition of cycles due to the increasing temperature of the sliding interface produced by frictional heating,
4. velocity effect - the gradual increase of μ with the increasing sliding velocity (Fig. 7).

One of the most relevant futures of the FP bearing is that residual displacements are reduced due to self-centering action induced by the concave spherical surface. Furthermore, the ultimate displacements can be increased simply by increasing the outside diameter of the spherical surface.

The reliability of dynamic and sliding properties of FP bearing has been verified experimentally and presented in works, among others in (Refs 19, 22-23).

3. ADAPTIVE SLIDING SUPPORTS

To avoid the possibility of resonance of the FP bearing with long predominant periods of ground motions a purely passive adaptive bearings have been proposed. An adaptive seismic isolation system is capable of change the stiffness and damping during its operation.

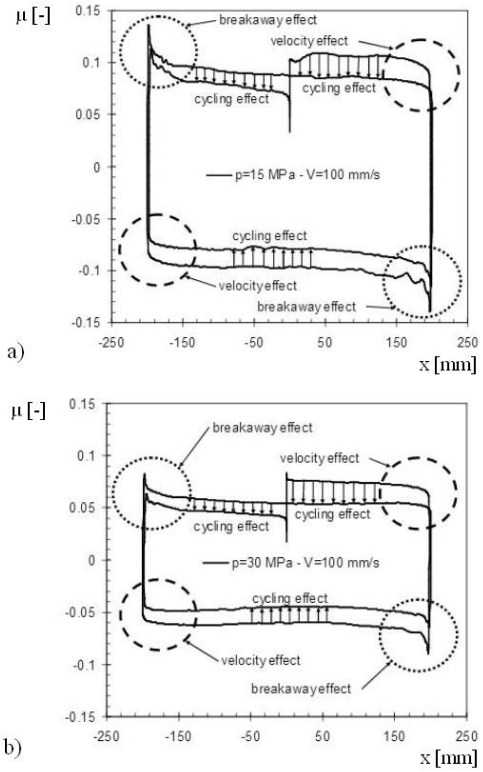

Fig. 7 Frictional coefficient-displacement loop from tests with V=100 mm/s for: a) p=15 MPa (W=3263 kN), b) p=30 MPa (W=6525 kN) (Ref. 22)

By adaptive behavior, it meants that stiffness and effective friction change to predictable values at calculable and controllable displacement amplitudes. Adaptive bearings exhibit different hysteretic properties at different displacement phases. Friction pendulum bearing we call adaptive when its stiffness and friction change in proportion to the displacement amplitudes at which the FP bearing is operated.

This property allows to design isolation systems for many different levels of excitation and for many different response purposes.

There are three types of passive adaptive FP bearing:

1. sliding isolators with multiple sliding surfaces (SIMSS),
2. sliding isolators with variable curvature (SIVC),
3. sliding isolators with variable friction (SIVF).

The SIMSS isolator includes supports with more than one sliding surface. Due to different arrangement of many sliding surfaces, these isolators are able to adapt to larger displacements of the isolator with its smaller geometrical dimensions. Isolators from the second group (SIVC) have an isolating adaptive rigidity that constantly changes, along with the displacement of the isolator. By describing the sliding surface, the SIVC's restoring force an isolation became designable parameters. In the case of variable friction isolators (SIVF), the sliding surface can have a constant radius but the friction coefficient of the isolator is a function of its displacement, which leads to an adaptive damping that changes with the displacement of the isolator.

3.1. Sliding isolators with multiple sliding surfaces (SIMSS)

The multi-stage FP bearing as compared to the single FP bearing has greater design flexibility, since the length of the pendulum and the coefficient of friction are determined for each independent pendulum mechanism.

Currently there are three types of multi-concave FP bearings (Fig. 8):
1. double concave friction pendulum (DCFP) bearings,
2. triple concave friction pendulum (TCFP) bearings,
3. quintuple concave friction pendulum (QCFP) bearings.

Each of them is an improved version of the previous one. The main difference between them is the number of slip surfaces.

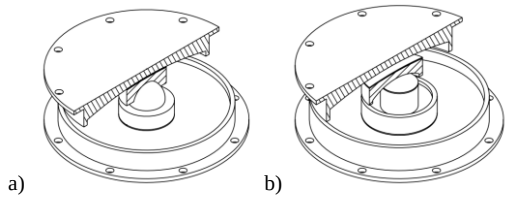

a) b)

Fig. 8 View of the: a) DCFP bearing, b) TCFP bearing (Refs 24-26)

In the case of double-concave FP bearing, the parameters characterizing its cyclic behavior are: R_1 i μ_1 for one concave sliding interface, R_2 i μ_2 for the second and h_1 i h_2 distance of one and the other sliding surface from the bearing center and d_1 i d_2- displacement capacities - for one and the other curved surface, respectively (Fig. 9) (Ref. 24).

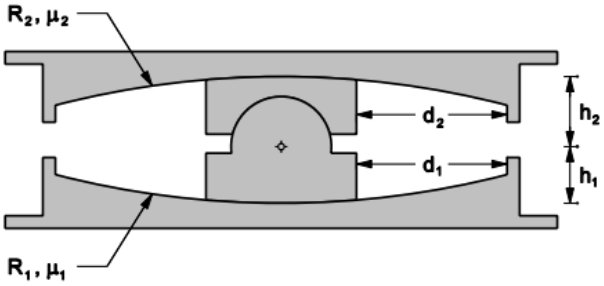

Fig. 9 Cross section of the DCFP bearing with surfaces of equal displacement capacity (with an articulated slider) (Ref. 24)

In comparison to single FP (SFP) bearing, double-concave FP (DCFP) bearing is characterized by a greater number of parameters describing the force-displacement relationship that the designer can control.

Based on experiments, it has been proven that using the curved surfaces with different radius of curvature and different coefficients of friction, a rigid-trilinear histeretic relationship can be obtained by using the upper and lower plates with different displacement (Fig. 10) (Ref. 24).

Assuming that the coefficients of friction differ on curved surfaces, the Double FP bearing behavior includes the following three slip steps (Table 1 and 2):

1. initial slip only on the surface with the lowest coefficient of friction,
2. then, simultaneous sliding on both surface of friction over the surface of higher friction,
3. sliding on only one surface after the displacement restrainer is contacted on the other.

Table 1. Summary of DCFP bearing behaviour (Refs 24-26)

Stage	Force-Displacement Relationship
Stage I: Sliding initiates on surface 1 but external force cannot overcome the friction on surface 2	$F = \frac{W}{R_{eff1}} x + F_{f1}$
Stage II: External force overcomes the friction force along surface 2; sliding occurs on both surfaces	$F = \frac{W}{R_{eff1} + R_{eff2}} x + + \frac{F_{f1} R_{eff1} + F_{f2} R_{eff2}}{R_{eff1} + R_{eff2}}$
Stage III: Slider contacts displacement restrainer on surface 2 and continues sliding on surface 1	$F = \frac{W}{R_{eff2}} (x - d_1) + F_{f2}$
Assumption: $(1)\ \mu_1 < \mu_2, \quad (2)\ d_1 < \frac{R_{eff1}}{R_{eff2}} d_2 + (\mu_2 - \mu_1) R_{eff1}$	

Table 2. Description of DCFP bearing design parameters (Refs 24-26)

Parameters	Description	Equation
R_{eff1}	Effective radius of curvature related to surface 1	$R_1 - h_1$
R_{eff2}	Effective radius of curvature related to surface 2	$R_2 - h_2$
T_I	Period of system during first stage of sliding	$T_I = 2\Pi\sqrt{R_{eff1}/g}$
T_{II}	Period of system during second stage of sliding	$T_{II} = 2\Pi\sqrt{R_{eff1} + R_{eff2}/g}$
T_{III}	Period of system during third stage of sliding	$T_{III} = 2\Pi\sqrt{R_{eff2}/g}$

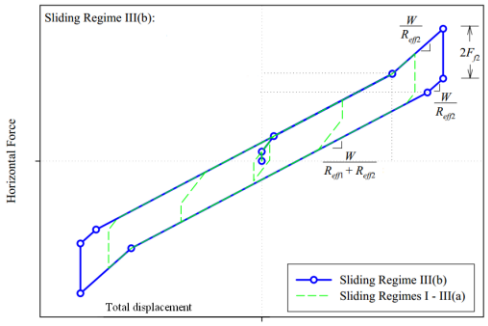

Fig. 10 Force-displacement relationship for sliding regime III (b) in comparison to sliding regime I÷III(a) (Ref. 25)

DCFP bearing with one surface with low coefficient of friction and a small radius in the set with the other surface with a large radius and high coefficient of friction has better re-centering capabilities for weak excitations, but still has sufficient stiffness and ability to dissipate larger excitations (Ref. 24).

M. Malekzadeh and T. Taghikhany (Refs 27-28) studied the seismic behavior of structures supported by DCFP bearings and the structure isolated only by single FP bearings. The results obtained by them confirm the advantages of DCFP bearings, acting as an adaptive isolation system, where stiffness and attenuation vary depending on the input level of ground vibrations and can control the acceleration peak and the interstory drift (Ref. 27).

The main advantages of DCFP bearing are: reduction of thermal effects, increase of displacement abilities compared to FP bearing for given cross-section dimensions, its compact dimensions, which translates into a reduction of costs. An important difference between FP bearing and DCFP bearing is the internal bending moment induced by the vertical load applied when the isolator is in a displaced configuration. In the case of DCFP bearing, both structures below and above the isolator should be designed to take over the bending moment. In the case of a standard FP bearing, depending on whether the support is downward or upward, the bending moment arises only on one side of the isolator.

Another FP bearing, an improved version of the previous ones, with adaptive behavior is the triple-concave FP (TCFP) bearing with four sliding surfaces, two sliding plates and a rigid slider (Figures 11 and 12) (Ref. 25). Its adaptive behavior results from various slip combinations that can occur on its many curved surfaces. The above adaptive bearing can be designed to take on different displacement sizes by simply correcting the curvature and radius of the surface. When the surfaces followed by slipping change, stiffness and friction also change (Ref. 24).

Fig. 11 Concaves and slider components of the TCFP bearing (Ref. 17)

Different stages of sliding related to TCFP bearing are as following (Fig. 13):

- Stage I: Sliding on surface 2 and 3 only,
- Stage II: Motion stops on surface 2, sliding on surface 3,
- Stage III: Motion stopped on surface 2 and 3, sliding on surface 1 and 2,
- Stage IV: Slider contacts restrainer on surface 1, motion remains stopped on surface 3, sliding on surface 2 and 4,
- Stage V: Slider bears on restrainer of surface 1 and 4, sliding on surface 2 and 3.

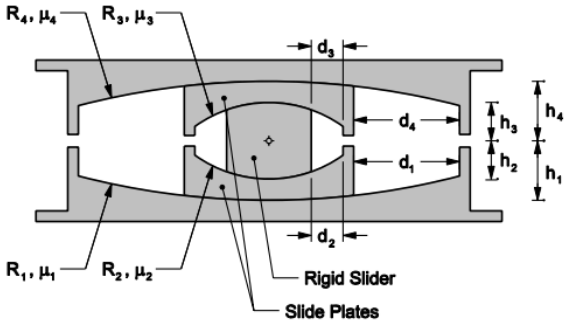

Fig. 12 Cross section of the TCFP bearing (Ref. 24)

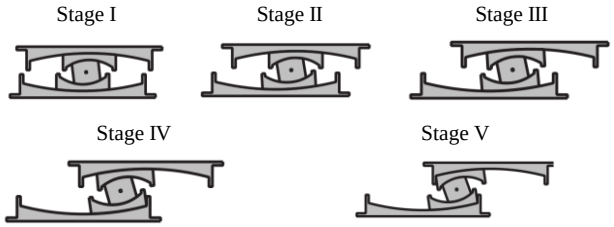

Fig. 13 Different stages of sliding related to TCFP bearing (Ref. 25)

Figure 14 shows the hysteresis loop for TCFP bearing with the following assumptions (Ref. 29):

a) $R_{eff2} = R_{eff3} \ll R_{eff1} = R_{eff4}$,

b) $\mu_2 = \mu_3 < \mu_1 < \mu_4$,

c) $d_2 > (\mu_1 - \mu_2)R_{eff2}$,

d) $d_3 > (\mu_4 - \mu_3)R_{eff3}$.

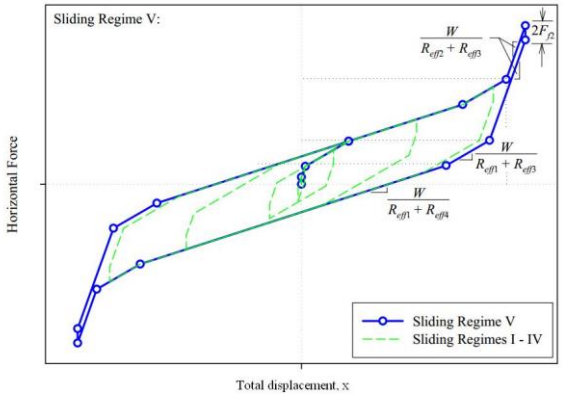

Fig. 14 Force-displacement relationship for TCFP bearing during sliding regime V shown in relation to sliding regimes I-IV (Ref. 25)

Numerical study (Ref. 30) of TCFP bearing shows that isolator with friction controlled in proportion to displacement amplitude significantly enhances the isolation of the structure. Hence the authors conclude that displacement amplitude proportional friction is seen as the objective function for the future development of passive adaptive pendulums. The quintuple-concave FP (QCFP) bearing (Ref. 25), which is at the present the latest version of the multi-concave FP bearing, has a stiff slider and six curved surfaces. Fig. 15 shows a cross section of QCFP bearing, and Fig. 16 shows a force-displacement relationship during sliding regime IX for this support.

Table 3 shows further improved versions of FP bearing and basic information about them. The increase in the number of pendulums and slip stages increases the ability of the adaptive behavior of the support at the expense of increased complexity in modeling its behavior. The number of effective pendulums means the name of the support (Ref. 29).

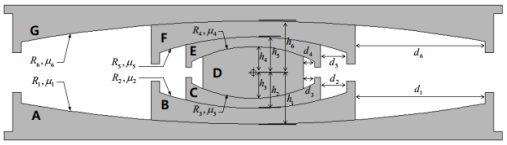

Fig. 15 Cross section of quintuple friction pendulum isolator (Ref. 25)

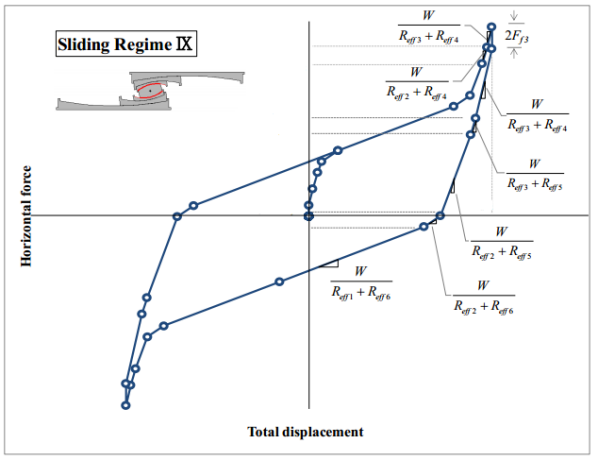

Fig. 16 Force-displacement relationship for QCFP bearing during sliding regime IX (Ref. 29)

To enhance the quakeproof efficiency and reduce the size of the FP bearing an interesting multiple friction pendulum systems (MFPS) was proposed among others by Tsai at all (Ref. 31) and K. Nishimoto at all 2017 (Ref. 32).

Table 3. Evolution of friction pendulum isolator and number of effective pendula and sliding regimes (Ref. 29)

	Configuration	Number of effective pendula	Number of sliding regimes
Single FP		1	1
Double FP	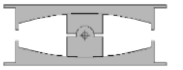	2	3
Triple FP	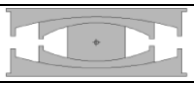	3	5
Quintuple FP	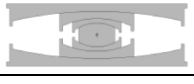	5	9

The response of multi-phase supports is characterized by the final stage of stiffening, which causes gradual transfer of forces to the superstructure, reduction of impact (at a sufficiently long reinforcement phase) and significant reduction of speed when the impact occurs at the level of isolation (Ref. 33).

The key role in the response of the design with multi-concave friction pendulum bearings plays the displacement capacity of bearings. Multi-surface devices can be potentially designed for different earthquake magnitudes.

3.2. Sliding isolators with variable curvature (SIVC)

The Variable Frequency Pendulum Isolator (VFPI) has the advantages of PF and FP isolators due to the amplitude dependent time and the mechanism reducing the bearing resistance force. This device is relatively flatter than FP bearing and hence is characterized by smaller vertical displacements. The flat surface will cause lower inversion forces in the structure.

With a low level of excitation, the behavior of the VFPI is similar to the behavior of FP bearing for smaller displacements (with the desired initial high stiffness). With a high level of excitation, the behavior of VFPI is similar to the behavior of PF bearing, for very large displacements (with large sliding displacement but without significant residual displacements). In order to achieve high efficiency of this device, the changing frequency is kept at every level of excitation. The effect of the isolator's pendulum will provide the necessary restoring force. The VFPI geometry is a modification of the ellipse equation:

$$y = b\left[1 - \frac{\sqrt{d^2 + 2dx\,\mathrm{sgn}(x)}}{d + x\,\mathrm{sgn}(x)}\right]. \tag{6}$$

The frequency of the isolator is given in the form:

$$\omega^2(x) = \frac{\omega_i^2}{(1+r)^2\sqrt{1+2r}}. \tag{7}$$

where: $\omega_i^2 = gb/d^2$ is square of initial frequency of the isolator (at zero displacement); b and d are geometrical parameters of VFPI; $r = x\,\mathrm{sgn}(x)/d$; x is the isolator displacement at any instant (Ref. 34).

VFPI is less effective under the action of near-fault ground motion and low frequency ground motion, because the sliding displacements they are too big.

Variable Radius Friction Pendulum System (VRFPS) was proposed by Krishnamoothy [35-36] to the isolation of spatial frame structures and then modified and applied to bridge isolation. The VRFPS geometry was selected in such a way that the radius was similar to the FP bearing, at the center of the slip surface, and increased along with the sliding movement and remained unrestricted on large displacements. The expression describing the radius of curvature that changes exponentially with the sliding displacement is:

$$R(x) = C[\exp(x) - 1] + R. \tag{8}$$

where C is the parameter to describe the variation of curvature of the concave surface, x is a sliding displacement expressed in meters, R is the radius of curvature in meters at the center of VRFPS (at x+0).

Geometry of the sliding surface is obtained as

$$y(x) = \int \frac{x\,dx}{C[\exp(x) - 1] + R}. \tag{9}$$

The isolator frequency and the isolator stiffness can be expressed by the following equations:

$$\omega = \sqrt{\frac{q}{R(x)}}, \qquad K = m\frac{q}{R(x)}. \tag{10}$$

At low displacement values (x), the behavior of VRFPS is similar to the behavior of FP bearing and at very large displacements, the VRFPS behavior is similar to the behavior of PF bearing. The value of C can be determined based on the analysis of the advantages of both PF and FP bearings.

VRFPS does not experience any resonance problems that occur in FP bearings for near-fault earthquake ground accelerations. VRFPS slip movements are larger than for FP bearings, due to the relatively flatter VRFPS surface compared to FP bearings on large slip displacements.

The effectiveness of a hybrid system consisting of VRFPS and passive VFD (Viscous Fluid Damper) to isolate the bridge structure was examined by A. Krishnamoorthy for different values of the attenuation coefficient VFD (Ref. 36).

By adding a passive VFD to the VRFPS, the sliding displacements were significantly reduced and the efficiency of the system increased. Like FP bearing, VRFPS is effective in bringing the structure to its initial position after the earthquake (Ref. 37).

Conical Friction Pendulum Isolator (CFPI).

The CFPI slip surface is identical to the FP bearing surface (with constant radius) when the isolator displacement is within the threshold values of $\pm d_b$. When the displacement of CFPI exceeds d_b, the slip surface is tangential to the spherical surface. The CFPI geometry is in the form:

$$y(x) = \begin{cases} R - \sqrt{R^2 - x^2}, & |x| \le d_b \\ c_1 + c_2(|x| - d_b,) & |x| > d_b, \end{cases}, \tag{11}$$

where: $c_1 = R - \sqrt{R^2 - d_b^2}$, $c_2 = d_b / \sqrt{R^2 - d_b^2}$.

The isolation frequency shown as:

$$\omega(x) = \sqrt{\frac{K(x)}{m}} = \sqrt{q\,y''(x)}, \tag{12}$$

where: $K(x) = mqy'' = mq\kappa(x)$ is restoring stiffness of the isolator; m is the total mass of the isolator structure; κ(x) is the curvature of the curved surface: $[\kappa(x) \cong y''(x) \quad \text{when } y'(x) \ll 1]$.

Hysteresis-loop diagram (force-displacement diagram) of isolator is in the form:

$$F(x) = W[y'(x) + \mathrm{sqn}(\dot{x})\mu], \tag{13}$$

where: W is the vertical load applied on the slider, x is the projection of unbalanced resultant force tangent to the surface on the x-coordinate (horizontal coordinate).

This the isolation system possesses no predominant frequency when the isolator displacement exceeds d_b:

$$\omega(x) = 0 \quad for \quad x > d_b, \tag{14}$$

and restoring force becomes a constant when the isolator displacement exceed d_b:

$$F_r(x) = W\,y'(x) \quad \text{for} \quad x > d_b, \tag{15}$$

and therefore the isolator behaves like PF bearing.

Polynomial Friction Pendulum Isolator (PFPI) was suggested by L.Y. Lu at all to eliminate the resonance problem associated with FP bearing. The bearing has an axially symmetric surface with a variable curvature and thus the isolation frequency becomes a displacement function. The geometric function of the sliding surface is defined by the following sixth-order polynomial (Refs 38-39):

$$y(x) = 1/6\,a\,x^6 + 1/4\,c\,x^4 + 1/2\,e\,x^2, \tag{16}$$

where: a, c and e are constant coefficients describing the mechanical behavior of the PFPI.

Restoring force normalized with respect to the vertical load W can be written as:

$$y'(x) = F_r(x)/W = a\,x^5 + c\,x^3 + e\,x. \tag{17}$$

Normalized isolator stiffness can be defined as:

$$y''(x) = K(x)/W = 5ax^4 + 3cx^2 + e \ . \tag{18}$$

Polynomial coefficients: a, c, e are calculated on the basis of the following equations:

$$y''(0) = k_0, \quad y'''(D_1) = 0, \quad y''(D_1) = k_1, \tag{19}$$

where: k_0 is the normalized initial stiffness at x=0; D_1 is the normalized isolator stiffness at x=D_1 and D_1 is the critical isolator drift, after which the PFPI system will switch from the acceleration control to displacement control.
The main feature of this isolator is that it has a weakening section (a softeninig section) followed by a hardening section. The weakening section accordingly reduces the response level of the acceleration, while the reinforcing section reduces the isolator drift and secures system stability during strong earthquakes. Numerical studies confirmed the high efficiency of PFPI, which is able to reduce the isolator drift and accelerate the structure in parallel (Ref. 38).

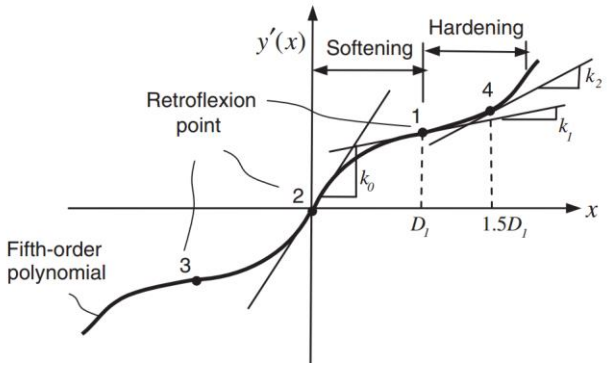

Fig. 17 Normalized restoring force (Ref. 39)

Figure 17 shows the relation force - displacement for PFPI.
Another interesting type of SIVC bearing is the bearing proposed by Gilich et al. (Ref. 40) with an area based on a polynomial function of superior order. The curve equation that describes the sliding surface is:

$$y(x) = a\,x^b \ . \tag{20}$$

Parameters used to control the level of construction oscillation are friction coefficient μ and two values characterizing the curve - a and b.
Theoretical studies indicate that the slip surface based on polynomials of a higher order than 2 can provide decoupling at lower forces due to lower slope. Experimental studies show that an increase in the excitation frequency leads to more efficient isolation, and ensuring a low coefficient of friction, in order to achieve decoupling at low lateral (horizontal) forces (ie at early stages of the earthquake) is necessary. The disadvantage of isolators with variable curvature is that there is a need to place the elastic layer between a sliding surface and the slider (Ref. 40).
Another adaptive device is the **Variable Curvature Friction Pendulum System (VCFPS)**, similar to VFPI bearing. It was proposed by C.S. Tsai at all. The mechanical behavior of VCFPS is very similar to FP bearing. The difference between these isolators is that the radius of curvature of the VCFPS can increase with increasing curvature.
Thus, the basic period of vibration of the VCFPS structure can be shifted beyond the basic dominating periods near-fault ground motion, thus preventing resonance of the superstructure with the earthquake.
The concave sliding surface of the VCFPS is given as:

$$\begin{aligned} y &= R - \sqrt{R^2 - x^2} - f(x) \\ f(x) &= C\,\mathrm{sgn}(x_b)x^3 \end{aligned}, \tag{21}$$

where: R is the radius of curvature at the centre of the sliding surface of the VCFPS, x is the horizontal displacement of the isolator, f(x) is the function to describe the increase of the radius of curvature with an increase of the horizontal displacement and C is the parameter that describes the variation of curvature of the concave surface.
If the restoring force can bring the slider back to the center of the isolator within the range of the sliding displacement x_0, when with the following equation parameter C can be obtained:

$$C = \frac{W x_0 \Big/ \sqrt{R^2 - x_0^2} - T_0/\cos\Theta_0}{3W\,\mathrm{sgn}(x_0)x_0^2}, \tag{22}$$

where: W is the vertical loading resulting from the superstructure, T_0 is the quasi-static friction force, Θ_0 is the angle between the tangential direction of the concave sliding surface and the horizontal direction at the sliding displacement of x_0.
The fundamental period of the base-isolated structure with VCFPS can written as:

$$T = \frac{2\Pi}{\sqrt{\dfrac{g}{\sqrt{R^2 - x^2}} - \dfrac{\mathrm{sgn}(x)x\left(g\,x_0 \Big/ \sqrt{R^2 - x_0^2}\right) - g\tan\Theta_0}{\mathrm{sgn}(x_0)x_0^2}}}. \tag{23}$$

From the above equation, it follows that the basic period of the natural vibration of the isolated structure is prolonged with the increase of the isolator's displacement (Ref. 41).
Figure 18 shows the force-displacement relationship for three SIVCs in combination with the hysteresis loop for FP bearing.

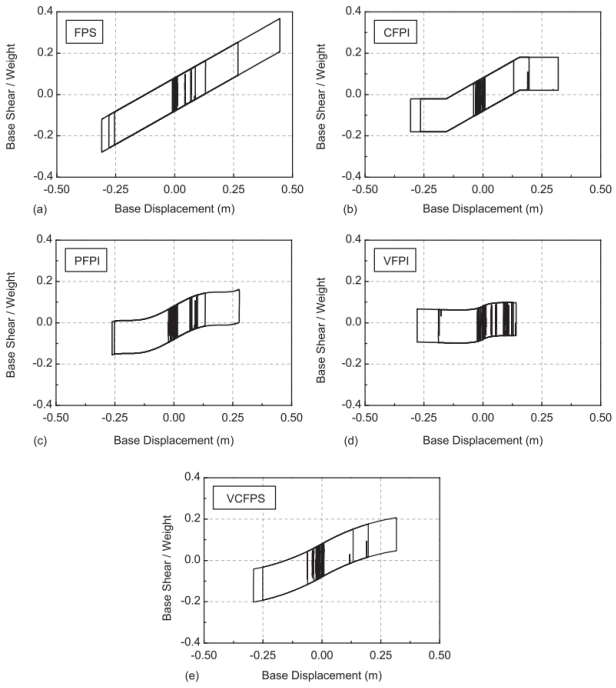

Fig. 18 Typical hysteresis diagrams of the four SIVC isolators under Jiji earthquake

3.3.Sliding isolators with variable friction (SIVF)
Variable Friction Pendulum System (VFPS) it is very similar in construction and operation to FP bearing.
The difference between VFPS and FP bearing is such that the coefficient of friction VFPS changes according to the curve, and the coefficient of friction FP bearing is a constant value (Fig. 19).

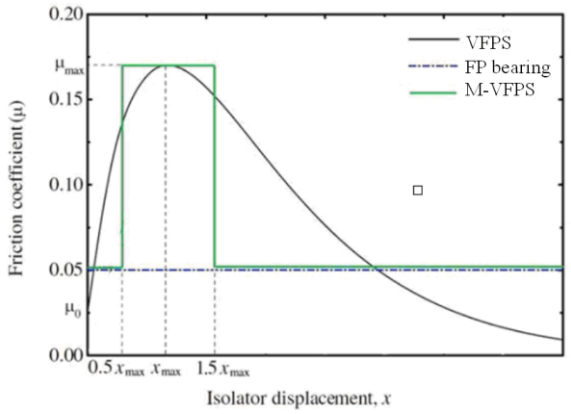

Fig 19 Comparison between friction coefficient of FP bearing, VFPS and M-VFPS (Ref. 41)

Such a change in the coefficient of friction in VFPS can be achieved by gradually varying the roughness of the spherical surface. The VFPS coefficient of friction is as follows:

$$\mu(x) = \left(\mu_0 + a_1|x|\right)e^{-a_2|x|}. \tag{24}$$

where: μ_0 is the initial value of friction coefficient, a_1, a_2 are the parameters that describe the variation of friction coefficient along the sliding surface and x is the isolator displacement.
The initial stiffnes K_i can be written as:

$$K_i = \frac{\mu_{max} W}{x_{max}}, \tag{25}$$

where: μ_{max} is the peak friction coefficient of the VFPS, x_{max} is the isolator displacement corresponding to peak friction coefficient, W=mg is the effective weight and m is the total mass of the base-isolated building. The value of x_{max} is calculated by maximizing $\mu(x)$ and is expressed as:

$$x_{max} = \frac{a_1 - \mu_0 a_2}{a_1 a_2}. \tag{26}$$

The initial time period T_i is as follws:

$$T_i = 2\Pi\sqrt{\frac{m}{K_i}}. \tag{27}$$

The restoring force is given by:

$$F = K_b\, x + F_x. \tag{28}$$

where: F_x is the frictional force, K_b is the stiffness of the VFPS.
The limiting value of the frictional force to which the VFPS can be subjected (before sliding) is expressed as:

$$Q = \mu W. \tag{29}$$

The stiffness of the VFPS is designed in such a way as to obtain a certain value of the isolation period expressed in the form:

$$T = 2\Pi\sqrt{\frac{m}{K_b}}. \tag{30}$$

VFPS modeling requires specification of two parameters - T and μ, and parameter μ can be defined by two parameters- T_i i μ_{max}.

The effectiveness of this system, applied to liquid storage steel tanks under the influence of trigonometric cycloidal pulses, was investigated and presented at work (Ref. 42).
The authors conclude that the seismic response of reservoirs near-fault ground motions can be controlled within a desirable range.
Modified Variable Friction Pendulum System (M-VFPS) was proposed by Shaihzadeh and Karamoddin [43-44]. The coefficient of friction in M-VFPS is identical to that in FP bearing except for the range 0,5 x_{max}÷1,5 x_{max} (x_{max} is defined as for VFPS).
The coefficient of friction μ is defined as follows:

$$\mu(x) = \begin{cases} \mu_{FP\,bearing} & 0 \le x \le 0{,}5\,x_{max} \\ \mu_{maxVFPS} & 0{,}5\,x_{max} < x < 1{,}5\,x_{max} \\ \mu_{FP\,bearing} & x > 1{,}5\,x_{max} \end{cases}. \tag{31}$$

In order to evaluate the effectiveness of M-VFPS, the authors compared the responses of two isolators (modeled with non-linear friction elements and variable spring elements) used in the 2-DOF shear building model.
In order to evaluate - base displacement and super-structural acceleration a set of seven near-fault earthquake excitations was considered.. The results indicate that the seismic behavior of M-VFPS is similar to VFPS, so M-VFPS can be treated alternatively. M-VFPS and VFPS are more effective in reducing base displacement compared to FP bearing, but they are not successful in controlling the acceleration transmitted to the superstructure.

4. CONCLUSIONS

Friction Pendulum bearings are widely used devices for the anti-seismic protection of buildings, bridges, industrial facilities, because of many advantages such as durability (in comparison with elastomeric bearings) and stability of mechanical properties. However, resonance problems can occur when the structure resting on friction pendulum bearings will be subjected near-fault earthquake ground motion characterized by low frequency and high intentensity. In order to overcome these problems, mechanical passive isolation systems were proposed by engineers improving friction pendulum bearing. There are three types of such isolators:

- with multiple sliding surfaces,
- with variable curvature,
- with variable friction.

These adaptive bearings are characterized by different hysteretic properties at different stages of displacement. Numerous studies confirm that these supports are capable of a stable performance under each type of earthquake, even in the case of near-fault ground motion.

REFERENCES

1. E. Aydin, B. Öztürk, M. Dutkiewicz: Analysis of efficiency of passive dampers in multistorey buildings, Journal of Sound and Vibration, Volume 439, p. 17-28,2019.
2. M. Dutkiewicz: Damping mass systems in the building structures, Logistyka, nr 6, 2010.
3. M. Dutkiewicz, I. Gołębiowska, I. Shatskyi, V. Shopa, A.Velychkovych: Some aspects of design and application of inertial dampers, MATEC Web of Conferences 178, 06010, IManE&E, 2018.
4. I. Gołębiowska, M. Dutkiewicz: Modelling of Flow Past Damper Attached to the Overhead Transmission Line, IOP Conf. Series: Materials Science and Engineering 245, 062054, 2017.
5. I. Gołębiowska, M. Dutkiewicz: The effectiveness of vibration damper attached to the cable due to wind action, EPJ Web of Conferences 143, 02029, WOS:000407743800031, 2017.
6. E. Aydın, B. Öztürk, M. Dutkiewicz, H. Çetin, O. Okkay, U. Ohancan, Y.E. Şirin: Experiments of tuned liquid damper (TLD) on the reduced shear frame model under harmonic loads, EPJ Web of Conferences 143, 02001, WOS:000407743800003, 2017.
7. E. Aydin, B. Öztürk, M. Dutkiewicz: Determination of optimal

elastic springs for cantilever beams supported by elastic foundation, Proceedings of 24th International Conference on Engineering Mechanics 2018, Web of Knowledge & Scopus, ISI Thomson Reuters, 2018, Svratka, Czech Republic.

8. I. Gołębiowska, M. Dutkiewicz: Experimental analysis of efficiency of mass dampers, Proceedings of 23th International Conference on Engineering Mechanics 2017, p.350-353, WOS:000411657600077, Svratka, Czech Republic.
9. E. Aydin, B. Öztürk, M. Dutkiewicz: Optimal passive control of shear buildings, Proceedings of 23th International Conference on Engineering Mechanics 2017, p: 98-101, WOS : 000411657600014, Svratka, Czech Republic
10. I. Gołębiowska M. Dutkiewicz: Use and efficiency of multiple mass dampers in construction foundations, Engineering Mechanics, Proceedings of 22th International Conference on Engineering Mechanics 2016, Web of Knowledge & Scopus, ISI Thomson Reuters, 2016, p. 166-169, WOS:000379986700038, ISBN: 978-80-87012-59-8, Svratka, Czech Republic.
11. Dutkiewicz M., Vibration of Euler-Bernoulli beam under random load carrying spring-mass system,: Proceedings of the 10th international conference "Computer systems aided science, industry and transport", TRANSCOMP, 2006.
12. I. Gołębiowska, M. Dutkiewicz: Vortex Induced Vibration and Wind Flow Around Bridge Cables, Springer Proceedings in Physics Volume: 198, p: 307-314, ISBN: 978-3-319-69823-6, 2018.
13. M. Dutkiewicz, V. Iancu, I. Gołębiowska: Passive Control Solutions Applied to Civil Constructions under Dynamic Load, Analele Universitatii 'Eftimie Murgu' , Vol. 24 Issue 1, p.101-112. 12p, 2017.
14. I. Gołębiowska, W. Sakiewicz: Base isolation systems in building structures. Engineering Mechanics 2014. Svratka, Czech Republic 12-15.05.2014. Engineering Mechanics, ISSN 1805-8248, p. 192-195, 2014.
15. I. Gołębiowska, M. Dutkiewicz, B. Usewicz: Devices of passive vibration control of building structures. Monograph from Scientific Seminar: Lightweight Structures In Civil Engineering. XXII LSCE - Olsztyn. s. 9-14, 2016.
16. V.A Zayas, S.S. Low, S.A. Mahin: The FPS earthquake resisting system experimental report. Technical Report UBC/EERC-87/01, 1987.
17. http://www.earthquakeprotection.com/pdf/EPSProductBrochure4PageVersionE.pdf.
18. Petti, F. Polichetti, A. Lodato, B. Palazzo: Modelling and analysis of base isolated structures with friction pendulum system considering near fault events; Open Journal of Civil Engineering Vol. 3, No. 2, 2013.
19. S. Barone, G.M. Calvi, A. Pavese: Experimental dynamic response of spherical friction-based isolation devices. Journal of Earthquake Engineering, 2017.
20. M. Kumar, A.S. Whittaker, M.C. Constantinou: Characterizing friction in sliding isolation bearing. Earthquake Engineering & Structural Dynamics, 2014.
21. G. Lomiento, N. Bonessio, G. Benzoni: Effects of loading characteristics on the performance of sliding isolation devices. 15th World Conference on Earthquake Engineering Lisboa, 2012, Vol. 26, pp. 20408-20417.
22. V.A. Zayas, S. Low, A. Mahin: A simple pendulum technique for achieving seismic isolation. Earthquke Spectra 1990, 6 (2), pp. 317-333.
23. D. Cordone G. Gesualdi: Influence of residual displacements on the desing displacement of spherical friction-based isolation system. Soil Dynamics Earthquake Engineering 2017, 100, pp. 492-503.
24. D.M. Fenz, M.C. Constantinou: Behavior of the double concave Friction Pendulum bearing. Earthquake Engineering and Structural Dynamics, 2006.
25. D.M. Fenz, M.C. Constantinou: Spherical sliding isolation bearings with adaptive behavior: Theory. Earthquake Engineering and Structural Dynamics 2008; 37(2):163-183.
26. D.M. Fenz, M.C. Constantinou: Modeling triple friction pendulum bearings for response history analysis. Earthquake Spectra 2008; 24(4):1011-1028.
27. M.Malekzadeh, T.Taghikhany: Adaptive behavior of double concave friction pendulum bearing and its advantages over friction pendulum systems. Civil Engineering Vol. 17, No. 2, 2010, pp. 81-88.
28. H. Moeindarbari, T. Taghikhany: Optimum Design of Triple Friction Pendulum Bearing Subjected by Near-Field Ground Motions, 15 WCEE2012, Lisboa 2012.
29. D. Lee, M.C. Constantinou: Quintuple friction pendulum isolato behavior, modeling and validation. Technical report MCEER-15-0007, 2015.
30. F. Weber, J. Distl, Ch. Braun: Isolation performance assessment of adaptive behavior of triple friction pendulum. Journal of Civil Engineering Research 2017, 7 (1) pp. 17-33.
31. C.S. Tsai, Y.C. Lin, H.C.: Su Characterization and modeling of multiple friction pendulum isolation system with numerous sliding interfaces. Earthquake Engineering And Structure Dynamic, 2010, 39.pp.1463-1491.
32. K. Nishimoto, H. Nakamura, N. Wakita: Development of spherical sliding bearing. Nippon Steel & Sumitomo Metal Technical Report No. 115, 2015, pp. 127-132.
33. T.C Becker, Y. Bao, S.A. Mahin: Extreme behavior in a triple friction pendulum isolated frame. Earth Engineering Structure Dynamic, 2017.
34. M Pranesh, R. Sinha: VFPI: an isolation device for a seismic design. Earthquake Engineering and Structural Dynamics 2000; 29, 603-627.
35. A. Krishnamoorthy: Variable curvature pendulum isolator and viscous fluid damper for seismic isolation of structures. Journal of Vibration and Control 17, 2010, pp. 1779-1790.
36. A. Krishnamoorthy: Seismic control of continuous bridges using variable radius friction pendulum systems and viscous fluid dampers. International Journal of Acoustics and Vibrations 20 (1): 24-35, 2015.
37. L.Y. Lu, M.H. Shih, C.Y. Wu: Near fault seismic isolation using sliding bearing with variable curvatures, Proc. Of 13th World Conference on Earthquake Engineering, 2004, Paper No. 3264.
38. L.Y. Lu, T.Y. Lee,S.Juang, S. Yeh: Polynomial friction pendulum isolators (PFPIs) for building floor isolation: An experimental and theoretical study, Engineering Structures, Volume 56, November 2013, Pages 970-982.
39. L.Y. Lu, T.Y. Lee, S.W. Yeh: Theory and experimental study for sliding isolators with variable curvature. Earthquake Engineering And Structural Dynamics. 2011;40:1609–1627.
40. G.R. Gillich, V. Iancu, N. Gillich, Z.I. Korka, C.P. Chioncel, C. Hatiegan: Decoupling the structure from the ground motion during earthquakes by employing friction pendulums. International Conference on Applied Science (ICAS2017) IOP Conf. Series: Materials Science and Engineering 294, 2018.
41. C.S. Tsai, T.C. Chiang, B.J. Chen: Finite element formulations and theoretical study for variable curvature friction pendulum system. Engineering Structures 25, 2003, pp. 1719-1730.
42. V.R. Panchal, R.S. Jangid: Variable friction pendulum system for seismic isolation of liquid storage tanks. Nuclear Engineering and Design 238(6): 1304-1315, 2008.
43. A.A. Shaikhzadeh, A Karamoddin: Effetiveness of sliding isolators with variable curvature in near-fault ground motions. The Structura Design Of Tall And Special Buildings, 2015.
44. A.A. Shaikhzadeh, A. Karamoddin: Behavior of sliding isolators with variable friction under near-fault earthquakes. 7th International Conference on Seismology & Earthquake Engineering, 2015.